IJCRT.ORG ISSN : 2320-2882

INTERNATIONAL JOURNAL OF CREATIVE RESEARCH THOUGHTS (IJCRT)

An International Open Access, Peer-reviewed, Refereed Journal

Alkali-Silica Reaction In Ultra-High-Performance Concrete: Performance And Quality Control Measures

[1]Vikas mirok, [2]Er. Raj Bala, [3]Er. Hardeep Singh

[1] M. TECH Scholar, [23] Assistant Professor

[123]Department of Civil Engineering, JCDMCOE, Sirsa, India

Abstract

The Alkali-Silica Reaction (ASR) is a critical durability issue in Ultra-High-Performance Concrete (UHPC), potentially compromising its exceptional mechanical properties and long-term performance. UHPC has emerged as a strong competitor to Normal Strength Concrete (NSC) in several building industries. This research examines the effects of ASR on UHPC, and its fiber-reinforced versions (UHPFRC) compared with NSC. Mechanical properties, including compressive, flexural, and split tensile strength, were assessed over varying curing periods (7, 14, 28, 56, 90, and 180 days) to analyze the influence of ASR. The study highlights the role of fiber reinforcement and optimized mix designs in enhancing resistance to ASR-induced damage. Mixtures of recycled steel fibers, raw slag (RS), and untreated coal ash (CA) were developed for use in sustainable UHPCs. Accelerated ASR conditions (per ASTM C1260) and conventional water curing were both applied to the specimens during the curing process. In addition, they compare the mechanical strength of UHPFRC and NSC over curing periods of 28, 56, and 90 days, focusing on the effects of ASR and water curing. The results demonstrated that the incorporation of fibers, particularly steel fibers, significantly enhanced the mechanical properties of UHPC, including higher CS and FS, while reducing the risk of crack propagation and improving overall durability. The comparison with NSC further underscored the advantages of UHPC and UHPFRC, which consistently outperformed NSC across all strength categories, with CS reaching up to 161MPa at 90 days compared to the maximum 37.8MPa for NSC.

Index Terms: Alkali-Silica Reaction (ASR), Ultra-High-Performance Concrete (UHPC), Fiber-reinforced, Mechanical Properties.

1. Introduction

Concrete is a fundamental element in building and is recognized as the most extensively used construction material worldwide, mostly owing to its superior strength and the simplicity of its production from readily available natural resources [1,2]. Concrete encounters difficulties due to environmental factors while it's prevalent use. Temperature changes and moisture variations can induce cracking in concrete components and expedite other types of degradation [3]. A major durability issue for concrete buildings in many applications is the Alkali-Silica Reaction (ASR) [4]. Amorphous silica in some natural aggregates reacts with hydroxyl ions in

cement to form ASR [5-8]. The aggregates include chemically inert silica (SiO2) mostly structured as siloxane groups ($\equiv Si - O - Si \equiv$) in the form of quartz. Crystalline silica becomes amorphous hydrous silica (silanol group [$\equiv Si - OH$]) when its surface disorderliness makes it attractive to water [9]. Subsequently as shown in Equations 1 and 2 [10], the silica(s) tends to dissolve when exposed to highly concentrated hydroxyl ions. This is achieved by neutralizing the silanol groups ($\equiv Si - OH$) and subsequently the siloxane groups ($\equiv Si - O - Si \equiv$).

$$\equiv Si - OH + OH^- = Si - O^- + H_2O \quad (1)$$

$$\equiv Si - O - Si \equiv +2OH^- = 2Si - O - + H_2O \quad (2)$$

As the structures ($\equiv Si - OH, \equiv Si - O - Si \equiv$) progressively decompose, they concurrently attract the soluble alkali hydroxides, namely NaOH or KOH, found abundantly in the concrete pore solution [11]. The hydroxyl ions (OH^-) in the pore solution are supplemented by the calcium hydroxide, $Ca(OH)_2$, that is formed during the hydration of the cement. The first byproducts of the interaction between these siloxane groups ($\equiv Si - O - Si \equiv$) and hydroxyl ions are an alkali-silicate solution or a gel, depending on the moisture level (Equation 3). Equations 4 and 5 show that alkali silicate hydrate and water are formed when $Si - OH$ interacts with additional OH^- and alkali metals.

$$\equiv Si - O - Si \equiv OH^- + R^+(Na \text{ or } K) = \equiv Si - O - Na + H - O - Si \equiv \quad (3)$$

$$\equiv Si - OH + OH^- + Na^+ = \equiv Si - O - Na + H_2O \quad (4)$$

$$\equiv Si - O - Na + nH_2O = \equiv Si - O^-(H_2O)_n + Na^+ \quad (5)$$

In order to create an alkali-calcium-silicate hydrate gel, the calcium ions in the cement paste react with the hydrated alkali-silicate gel that has diffused through the aggregates [12]. Sourced from [13–15], Figure 1 depicts a simplified view of ASR chemistry in concrete buildings.

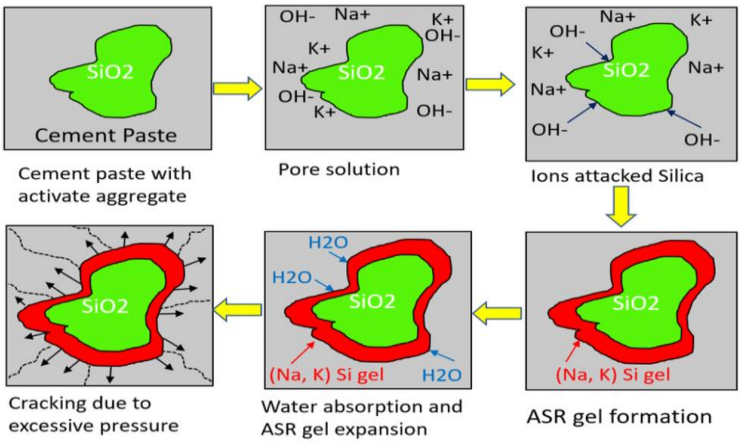

Figure 1: Processes and stages of ASR development in reactive aggregates used in concrete [16-18].

UHPC is a cementitious material that is relatively new and has exceptional strength, ductility, and durability. Concrete technologies such as HPC, fiber-reinforced concrete (FRC), and self-compacting concrete (SCC) could be used to create UHPC reinforced with fiber. Concrete with ductile behavior under stress and a typical CS of at least 150MPa is defined as a UHPC according to the French interim suggestions (AFGC 2002) [19]. Lower-strength UHPCs are those that have a CS between 130MPa and 150MPa and have been reinforced with steel or other fibers. A typical example of a UHPC would be a FRC, Super-plasticized (SP), silica fume-cement mixture with an extremely low water-to-cement ratio (W/C), where the fine quartz sand, with a size range of 0.15-0.60 mm, is utilized in place of the regular aggregate [20]. The benefits and applications of UHPC are shown in Figure 2.

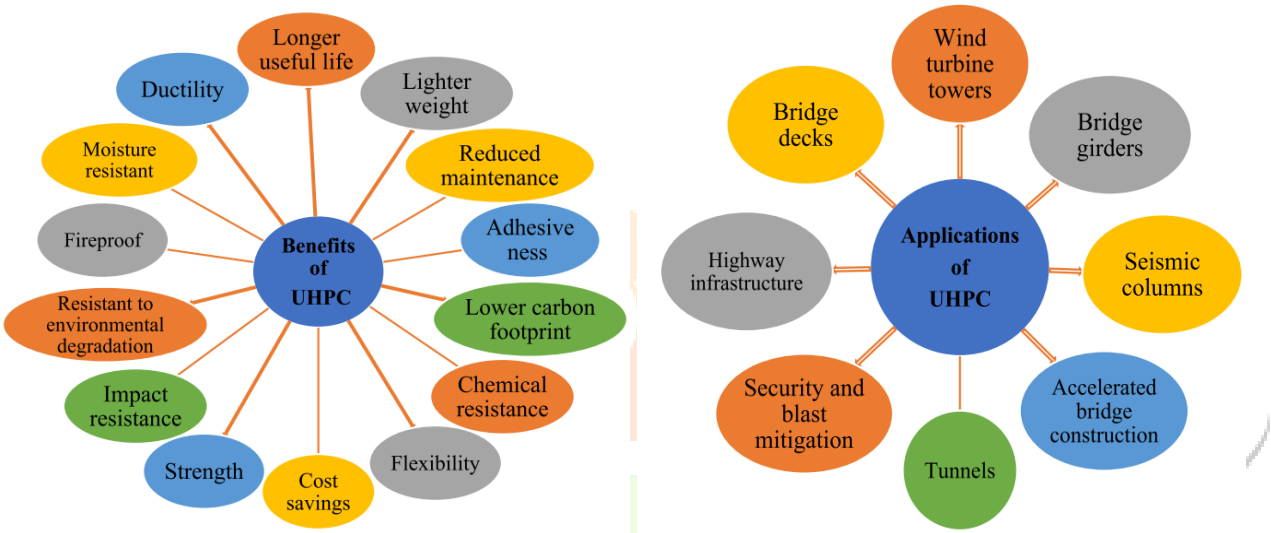

Figure 1: UHPC a) Benefits b) Applications [21].

The aim of the study based on the performance of ASR in UHPC. Here are some potential research objectives for a study follow as:

- Examine the chemical and physical characteristics of UHPC under ASR conditions.
- Identify effective supplementary cementitious materials (e.g., coal ash and raw slag) and their optimal proportions to reduce the risk of ASR.
- Examine the effects of mix design factors on ASR susceptibility in UHPC, such as aggregate grading and the water-to-cement ratio.
- Examine the impact of ASR on the mechanical parameters, including CS, FS, SPT and durability of UHPC.

2. Literature Review

In this section, the authors provide previous work based on the performance and quality control of ASR in UHPC with CS, FS, SPS.

UHPC is a novel cementitious material. The incorporation of waste glass with micro- and nanoparticles in UHPC has attracted considerable attention for its capacity to improve sustainability and material performance. In study [22], the authors examined the effects on UHPC characteristics of combining Micro-Waste (MG) and Nano-Waste Glass (NWG) with waste foundry sand. The findings show that the ideal CS is achieved by raising it by 11.6% after 7 days, 9.5% after 28 days, and 10.18% after 56 days when 20% MG is used in place of cement. Optimal CS at 1.5% replacement ratios of 17.5, 18.9, and 16% at 7, 28, and 56 days, respectively, is achieved by the efficient exploitation of NWG, which increases long-term resilience. STS increased 16% and 21% with 20% MG and 1.5% NWG respectively. The effects of different Ultrafine Fly Ash (UFA) contents on the microstructure, fiber pullout behavior, mechanical strengths, FS and STS, and 2 vol% steel fiber reinforced in Magnesium phosphate cement-based UHPC (MPC-UHPC) was suggested in [23]. The UFA concentration ranged from 0% to 15% by weight of binder. Incorporating 10%-15% UFA with an average particle size of 1.4 µm successfully reduced porosity and micro-cracks in the binder matrix and at the fiber-matrix interface, according to the experimental findings. Mixtures with 158.3MPa CS and significantly improved flexural and tensile fracture characteristics were produced by adding this amount of UFA.

In study [24], the researchers explored the possibility of using metakaolin (MK), pumicite, and Ground Granulated Blast-Furnace Slag (GGBFS) in place of cement, Fly Ash (FA), and SF in UHPC compositions. Workability, CS, and FS tests were performed on all mixes to select those that met the criteria for acceptable UHPC (28-day CS more than 120MPa). Findings shown that acceptable strengths could be achieved by substituting 25% pumicite, 100% metakaolin, and 40% GGBFS for the FA in the control mixture, respectively. For every combination, the FS was higher than 14.20 MPa. After have some limitation in previous work, the authors in work [25] used same industrial composites in place of cement to enhance the performance in UHPC compositions. To make the different mixes, researchers kept the SF quantity constant at 15% and played about with the proportions of Portland cement, GGBFS (30-50%), FA (20-30%), and MK (15-25%). The findings showed that the CS, FS, and STS were all enhanced with the addition of 15%MK. Additionally, the resistance to chloride permeability was improved. Ternary combinations of 50% GGBS and 25% MK had the lowest chloride-ion permeability resistance and mechanical qualities when compared with other mixtures.

In work [26], the investigators evaluated four novel UHPC combinations with alkali-activated material binder compared to a Portland cement mixture in terms of their environmental, material, energy, and water footprints. An alkali-activated UHPC has a 32%-45% larger efficiency in terms of a climate footprint and a 19%-33% better performance in terms of material footprints, but it comes at an obvious cost of 44%-83% higher energy footprints and 75%-146% higher water footprints. In study [27], the authors concentrated on using Recycled

Coarse Aggregate (RCA) to substitute 50% of the total Natural Coarse Aggregate (NCA). Two categories of replacements were employed: Carbon Nanofiber (CNF) at concentrations of 0.25%, 0.5%, 0.75%, and 1% by weight of the binder, and Steel Fibers (SFs) at concentrations of 0.5%, 1.0%, 1.5%, and 2% by weight of the binder. The CS was 151.3MPa for the NF0 combination and 146.9MPa for the RF0 mixture. The optimal enhancement in fiber-reinforced UHPC was recorded at 164.9, 158.6, 158.8, 153.5, 167.9, and 180.9MPa for the NCF0.5, RCF0.5, NSF2.0, RSF2.0, NCF0.25-SF2.0, and RCF0.25-SF2.0 mixes, respectively.

In study [28], the researchers examined the effects of micro-silica (MS) and SF on the mechanical properties of UHP-GP concrete. There were four distinct proportions of MS by total binder mass: 5%, 10%, 15%, and 25%; three different proportions of SF by volume: 0%, 1%, 2%, and 3%. There is an examination of the fracture energy, STS, CS, and FS. Evidence from this study demonstrates that UHP-GPC mechanical properties could be preserved while using less SF by increasing the concentration of MS.

3. Problem Formulation

The ASR poses a significant challenge to the durability and performance of concrete, particularly in UHPC. While UHPC offers exceptional strength and durability, its dense matrix and high cement content can exacerbate ASR due to the presence of reactive aggregates and alkalis. This reaction can lead to expansion, cracking, and a reduction in the long-term performance of the concrete. Despite advancements in UHPC formulations, there is a need for effective quality control measures to mitigate ASR and ensure structural integrity. The problem lies in balancing the high strength and durability benefits of UHPC with the risks of ASR while incorporating preventive strategies, such as the use of supplementary cementitious materials, optimized aggregate selection, and innovative testing techniques. This study focuses on analyzing the performance of UHPC, including fiber-reinforced variants (UHPFRC), in mitigating ASR through mechanical and durability assessments while proposing practical quality control measures to enhance long-term performance.

4. Material and Methods

Figure 3 illustrates the systematic workflow for studying the performance and quality control of ASR in UHPC. The selection of materials is a critical step, focusing on key components like cement, Coal ash (CA), and Raw slag (RS), which are analyzed for their chemical and physical properties to determine their suitability for UHPC. After selecting the materials, a mixture design for the tested UHPC is developed. This design phase ensures the proper proportions and characteristics of the materials to meet the desired performance standards. Subsequently, samples are prepared according to the established mixture design. These samples are subjected to a series of tests to evaluate their mechanical properties and resistance to ASR. The primary tests include CS, STS, and FS, alongside ASR testing to assess the durability and quality control aspects of the concrete. Finally, the results from these tests are analyzed to draw conclusions about the performance of the UHPC and its ability

to mitigate the effects of ASR. This systematic approach ensures a comprehensive evaluation of the material's properties and performance under various condition

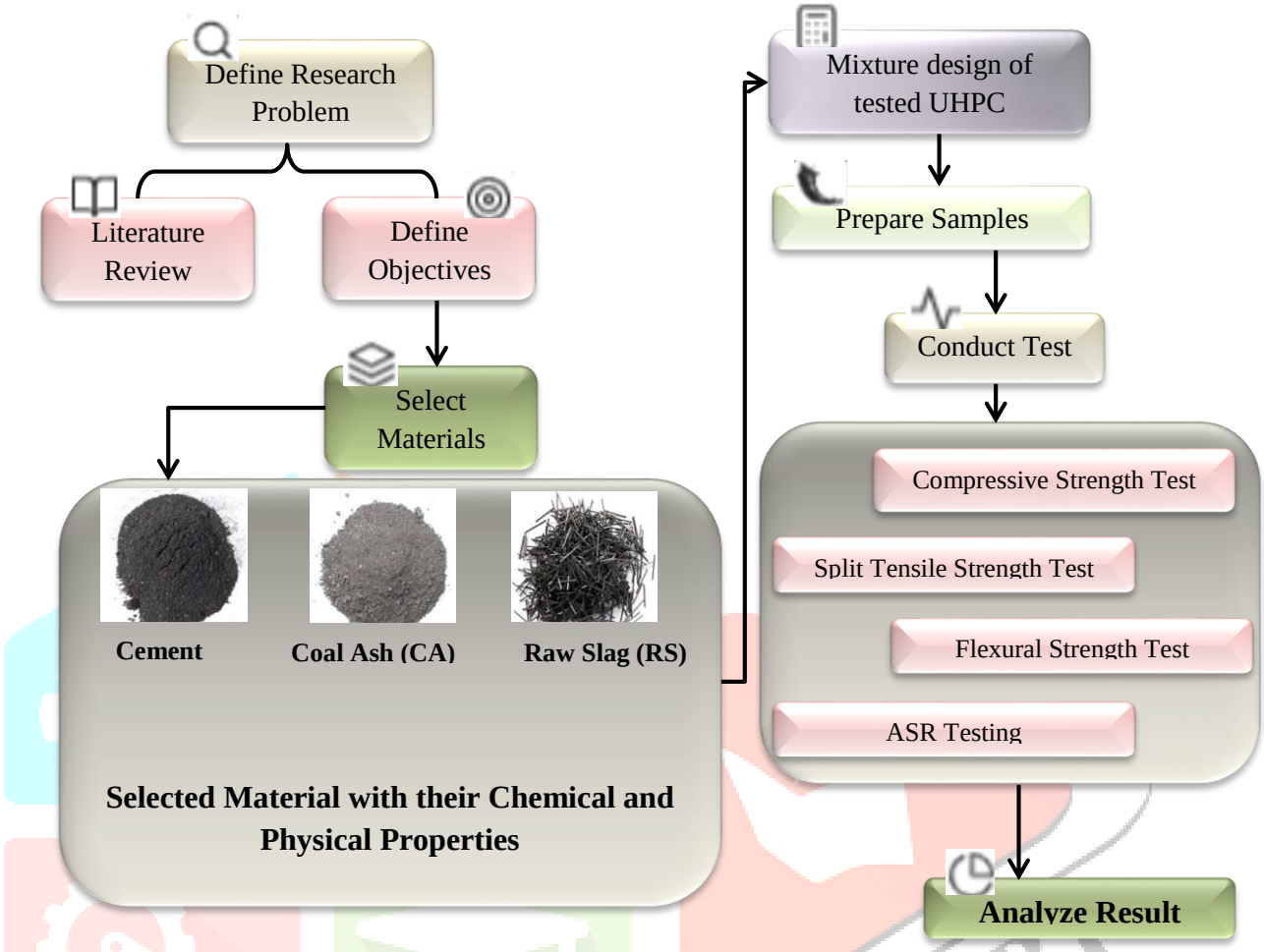

Figure 3: Flowchart of proposed work

4.1 Materials Used

It was constructed using ordinary Portland cement. CA that had not been treated was purchased from a thermal power plant in the locality. In addition, RS was obtained from the steel industry in the locality. Fibers with a length of 10mm were created by cutting lengthy steel wire that had been recycled (Figure 4).

a) b) c)

Figure 4: Raw materials used a) Cement b) Coal Ash c) Raw Slag

Analysis of the chemical composition of the cement, CA, and RS that was employed is shown in Table 1. The Loss on Ignition (LOI) was more than 10% for both the CA and the RS measurements. A comparison of the physical characteristics of utilized cement, CA, and RS is shown in Table 2. Silicon dioxide (SiO2) content of the silica sand was more than 98%, and it was sourced from the local glass industry. In addition, particles of quartz powder with grain sizes ranging from 450 to 500 microns were used. For the purpose of controlling the workability of mixes, a SP from polycarboxylate was added.

Table 1: The chemical characteristics of the raw materials that are utilized

Materials	Al_2O_3	SiO_2	Fe_2O_3	Mgo	CaO	SO_3	LOI
Cement (%)	4.56	21.05	6.34	3.12	61.06	3.82	3.92
CA (%)	13.34	37.43	5.62	2.53	10.45	4.67	12.06
RS (%)	12.15	33.54	5.72	0.67	8.62	33.51	11.75

Table 2: The physical characteristics of the raw materials that are utilized

Properties	Cement	CA	RS
Blaine Fineness (cm2/g)	3102	4412	4632
Fineness modules (%)	>96	>96	>96
Unit Weight (kg/m3)	1635	372	1294
Specific Gravity	4.11	3.42	3.26

The UHPC mixture designs that were tested are shown in Table 3. At first, a high-speed rotating shear mixer was used to dry mix the cement, CA, RS, and sand for duration of one minute. Wet towel was used to rinse the mixer bowl before adding the UHPC dry components. The mixture was gradually supplemented with half of the estimated water quantity. Subsequently, three more minutes of continuous high-shear mixing was performed after adding the remaining water and SP to the mixture. After the steel fibers were added, the mixture was mixed again until the fibers were evenly distributed and no longer clumped. The next step was to consolidate the specimens on a vibrating table after they had been prepared for analysis of CS and FS as well as STS. For each test, six copies were created at the required age in both cube and prism specimens. The specimens were put in a humid curing room with a temperature of 50◦C and a relative humidity of over 97% after being covered with plastic sheets. Specimens were removed from their molds after 24 hours and cured in water at 50◦C for a further 24 hours. Once the specimens were exposed, they were split into two groups. The cube and prism

specimens were immersed in a 1N NaOH solution at 80 ± 5◦C while the remaining specimens were cured in water at 20◦C±2.

Table 3: The tested UHPC mixture design

Ingredients	Cement Mass			
	UHPC1	**UHPC2**	**UHPFRC1**	**UHPFRC2**
Cement	2.56	2.56	2.56	2.56
Quartz sand	1.12	1.12	1.12	1.12
Silica sand	1.55	1.55	1.55	1.55
Fine sand	1.45	1.45	1.45	1.45
Raw slag	—	1.21	—	1.21
Untreated coal ash	1.21	—	1.21	—
Superplasticizer (SP)	0.45	0.45	0.45	0.45
Steel fibers	—	—	1.21	1.21

In addition, UHPC specimens were compared with Normal Strength Concrete (NSC) cube and prism specimens. The NSC specimens were prepared using rocks sourced from a nearby crush quarry. The ASTM C1260 criteria were followed for preparing the specimens, which included utilizing a cement-to-aggregate ratio ranging from 1 to 2.25 [29]. Specimen preparation also followed an aggregate grading scheme comparable to that of ASTM C1260. A ratio of 0.525 was used for the water to cement. All of the aforementioned curing protocols were applied to these NSC specimens as well.

4.2 Conducted Test

a) Compressive Strength (CS)

The CS was measured by utilizing 150 mm concrete cubes. Cubes of cast concrete are submerged in water to cure after 24 hours of casting. The specimens are subjected to compression testing at 7, 14, 28, 56, 90, and 108 days. Dividing the load at failure by the specimen's cross-sectional area provides the concrete's CS [30].

$$Compressive\ Strength = \frac{Load}{Cross-sectional\ Area} \quad (1)$$

b) Flexural Strength (FS)

The FS was used to assess the bending behaviour of the foamed concrete specimens at the maximum failure load [31]. At 7, 14, 28, 56, 90, and 108 days, the test was conducted. Over the rollers, the specimen was placed on the bottom plate. The specimen was subjected to a two-point force in the centre until it broke. The formula for determining flexural strength is [32]:

$$F = PL/bd^2 \quad (2)$$

In this equation, F stands for the concrete's flexural strength in MPa,

P for the failure load in N,

L for the beam's effective span in mm, and

b for the beam's width in mm.

c) Split-Tensile Strength (STS)

One of the most fundamental and significant characteristics of concrete is its tensile strength. In order to design concrete structural components that are susceptible to temperature, transverse shear, torsion, and shrinkage effects, and its value must be known. Its significance is also considered while designing liquid retaining structures, highways [33], runway slabs, and prestressed concrete structures. The specimen's STS can be determined by following equation [34]:

$$T = 2P/pi\ LD \quad (3)$$

In the above equation: T = Tensile strength upon splitting, measured in MPa,

P: The testing machine's maximum applied load as shown in N,

L: The specimen's length in millimetres and

D: The specimen's diameter in millimetres.

Table 4 displays the statistics for each test, including the number of specimens and the coefficient of variation (COV).

Table 4: Variance coefficients and sample numbers for different analyses

Mixtures	Days	No. of Specimens	CS		FS		STS	
			Water	ASR	Water	ASR	Water	ASR
UHPC1	28	6	2.13	2.56	1.90	1.76	2.56	2.34

	56	6	2.54	2.35	2.14	2.41	2.12	2.56
	90	6	2.34	2.14	2.21	2.48	2.74	2.62
UHPC2	28	6	2.32	2.41	1.78	1.92	2.25	2.38
	56	6	2.67	2.26	2.21	2.72	2.83	2.74
	90	6	2.84	2.94	2.34	2.47	2.10	2.31
UHPFRC1	28	6	2.84	2.72	2.33	2.98	2.58	2.43
	56	6	2.56	2.53	2.46	2.68	2.31	2.95
	90	6	2.93	2.85	2.64	3.10	2.93	2.80
UHPFRC2	28	6	2.57	2.58	2.76	3.05	2.84	2.87
	56	6	2.34	2.34	2.82	2.84	2.05	2.16
	90	6	2.92	2.87	2.91	2.95	2.64	2.42
NSC	28	6	2.74	2.77	3.15	3.23	3.14	2.27
	56	6	3.05	2.14	3.05	3.08	2.67	2.35
	90	6	2.67	3.06	3.24	3.19	3.83	3.74

4.3 Test Procedures

We used a flow table that was in line with ASTM C230 to test the flowability of new UHPC mixes [35]. Cube specimens of 50 × 50 × 50 mm were used to measure the CS of UHPC mixes, in accordance with ASTM C109 [36]. At a rate of 2.10MPa/sec, the specimens were loaded. Prism specimens of 40 × 40 × 160 mm were used to assess the FS of UHPC, following the guidelines of ASTM C348 [37]. When measuring FS, a loading rate of 2.85kN/min was established. In order to conduct the tests, specimens were removed from the ASR exposure and water curing conditions at the specified ages (7, 14, 28, 56, 90, and 108 days). An electronic length comparator was adjusted with the help of a reference rod in order to measure each expansion reading precisely. In order to get the expansion measurements, the ASTM C490 method was used [38]. To check for surface difficulty or cracking begin, each specimen was visually examined before testing.

5. Test Result and Discussion

The test findings derived from the experimental studies are provided as follows:

5.1 Flowability of UHPC

The evaluated UHPC mixes' flow statistics are shown in Table 5. Compared to the UHPC combination made using recycled sand, the one with coarse aggregate showed lower flow values. The decreased flow rate of the UHPC/CA blend was mostly caused by the significant ignition content loss, which includes unburned carbon and reduces the SP's efficacy. Coarse aggregate UHPC mixes exhibited decreased flow and higher water absorption after mixing because of their porous microstructure [39].

Table 5: Flow characteristics of evaluated UHPC mixes

Mixtures	UHPC1	UHPC2	UHPFRC1	UHPFRC2
Flow (mm)	191	197	173	180

However, the results show that, as predicted, the flowability of UHPC mixtures was decreased when SFs were added. SFs reduced the flowability of UHPC mixtures by about 10%. Possible alterations to the granular particles' skeletal structure are responsible for the reduced flow of UHPC mixtures containing steel fibers. This will result in heightened friction and blockage, impeding flow. Additionally, SFs serve as an impediment to diminish the flow velocity of new UHPC combinations [40,41]. Figure 5 show the graph of flow tested UHPC mixtures.

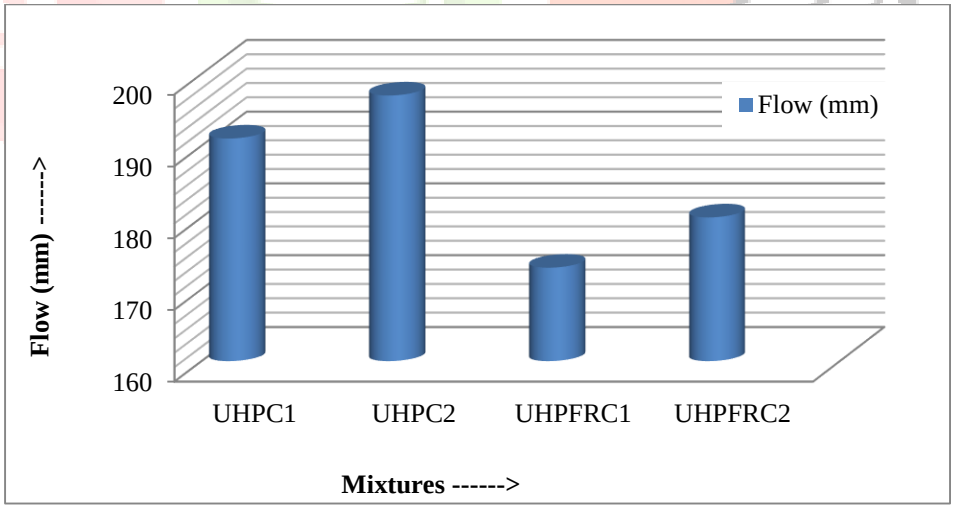

Figure 5: Flow of tested UHPC mixtures

5.2 Compressive Strength, Flexural Strength, and Split Tensile Strength

The performance and quality control of ASR in UHPC and its UHPFRC were assessed through CS, FS, and STS over curing ages ranging from 7 to 108 days. CS increased consistently for all mixes with time. Among the materials, UHPFRC2 demonstrated the highest compressive strength of 164MPa at 108 days, showcasing

superior performance due to fiber reinforcement. Conversely, UHPC1 exhibited the lowest compressive strength of 75MPa at 7 days, indicating slower early strength development.

FS followed a similar trend, with UHPFRC2 achieving the highest value of 29MPa at 108 days, highlighting enhanced resistance to bending due to fibers. In contrast, UHPC1 recorded the lowest flexural strength of 11MPa at 7 days.

For STS, UHPFRC2 again outperformed other mixes, reaching 10MPa at 108 days, which reflects excellent crack resistance and tensile behavior. UHPC1 had the lowest split tensile strength of 5.6MPa at 7 days. These results underscore the significant impact of fibers and curing time on the MS of UHPC, with UHPFRC mixes consistently outperforming UHPC mixes in terms of strength and durability across all tested parameters. Figure 6-8 show the graph of CS, FS, and STS.

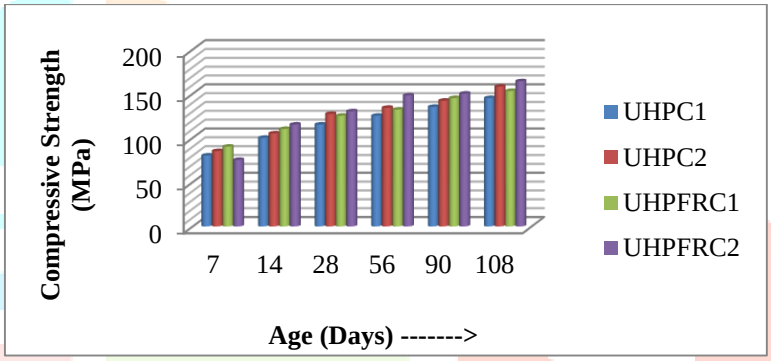

Figure 6: CS results

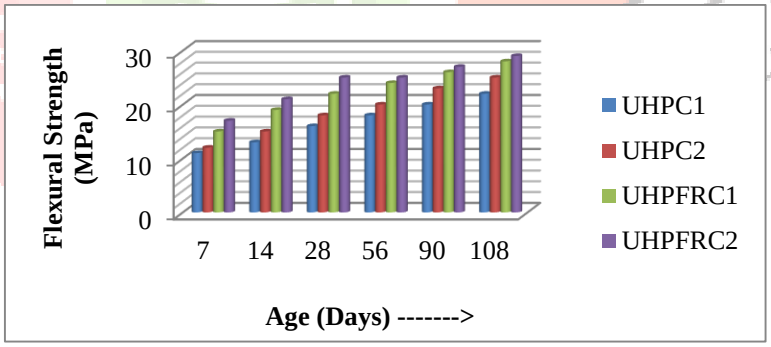

Figure 7: FS results

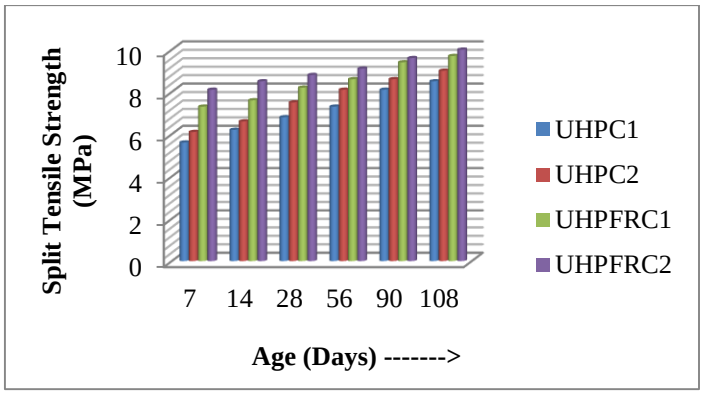

Figure 8: STS results

5.3 ASR Expansion Results

Figure 9 presents the ASR expansion graph for four types of ultra-high-performance concrete (UHPC1, UHPC2) and UHPFRC (UHPFRC1, UHPFRC2) over different curing ages. ASR expansion, a measure of durability and susceptibility to chemical degradation, is critical for assessing the long-term performance of these materials. At 7 days, UHPFRC2 exhibits the lowest ASR expansion (0.002%), followed by UHPFRC1 (0.006%), indicating superior resistance to ASR in fiber-reinforced concretes. In contrast, UHPC1 and UHPC2 show higher early-age expansions of 0.01% and 0.027%, respectively, reflecting a greater vulnerability to ASR due to the absence of fibers that enhance matrix integrity and crack resistance.

With increasing curing age, all mixtures show a gradual rise in ASR expansion, with UHPC1 and UHPC2 consistently exhibiting higher expansions compared to the fiber-reinforced variants. By 108 days, UHPFRC2 maintains the best performance with an expansion of 0.013%, followed by UHPFRC1 at 0.015%. UHPC2 and UHPC1 exhibit expansions of 0.126% and 0.13%, respectively, emphasizing the importance of mix design in controlling ASR. The data underscores the superior durability of UHPFRC mixtures, highlighting the effectiveness of fibers in mitigating ASR. Quality control measures, such as refined material selection and optimized mix proportions, are essential in minimizing ASR-related degradation and ensuring the long-term stability of ultra-high-performance concretes.

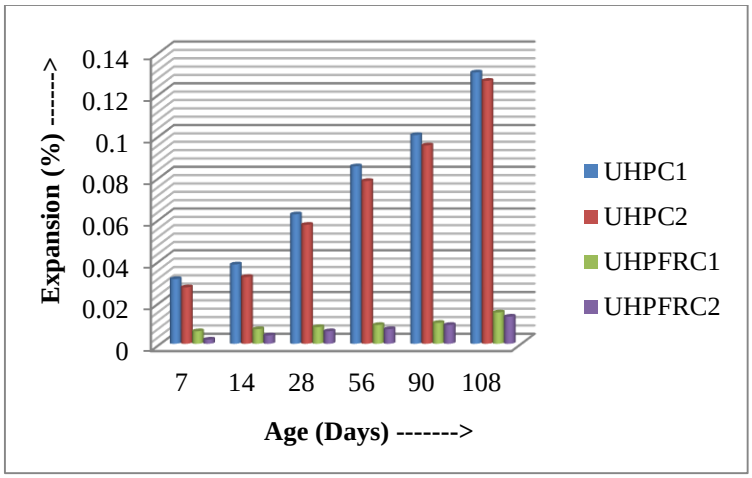

Figure 9: Expansion results for various UHPC mixtures

5.4 Impact of ASR Exposure on CS, FS, and STS

Figures 10-12 illustrate the effects of ASR exposure on the residual CS, FS, and the STS of UHPC mixtures over a period of 180 days. The data shows that both CS and FS increase with age for all the mixtures, regardless of ASR exposure. For CS, UHPC mixtures exposed to ASR demonstrate a slight reduction in strength compared to the control samples (UHP C1), with UHPFRC mixtures 1 and 2 exhibiting stronger resistance to ASR. The CS of these mixtures continues to increase over time, with minimal difference between mixtures exposed to ASR. In terms of FS, similar trends are observed, with the FS also increasing across all mixtures with age. Notably, the FS are relatively higher in the UHPC mixtures, with ASR exposure affecting only marginally over time. Additionally, the data on STS confirms that all mixtures experience gradual improvements in performance. The study emphasizes that although ASR exposure slightly impacts the overall mechanical properties of UHPC; the mixtures remain robust, highlighting the importance of quality control and the role of ASR mitigation strategies in preserving the strength and performance of UHPC over time.

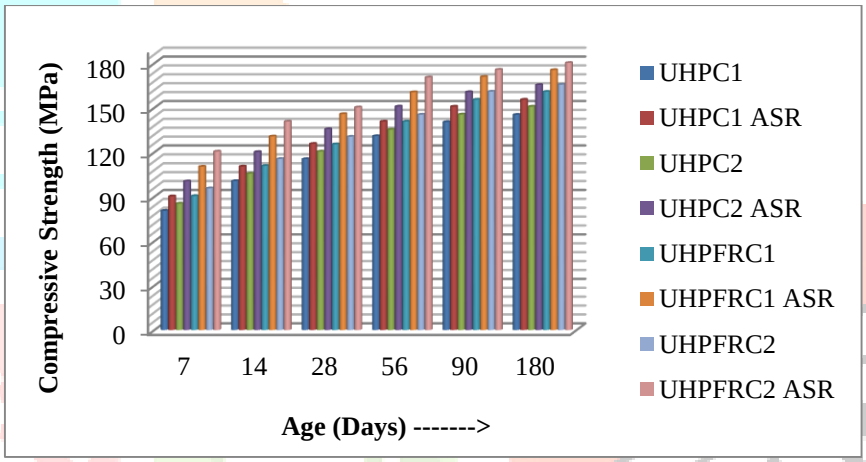

Figure 10: Compressive Strength

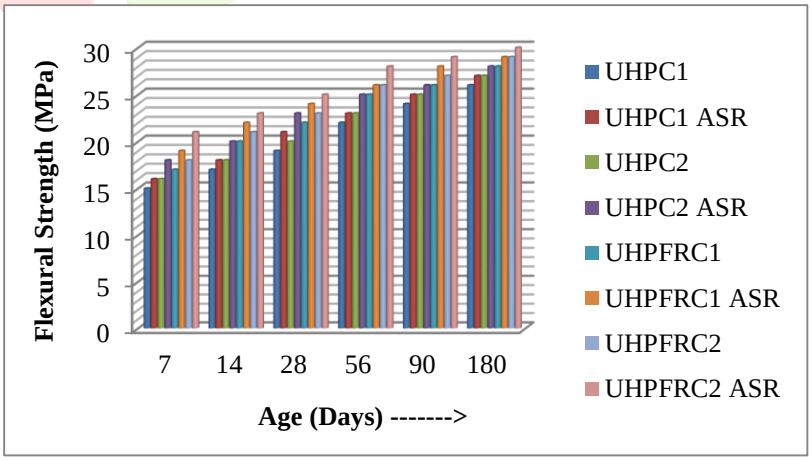

Figure 11: Flexural Strength

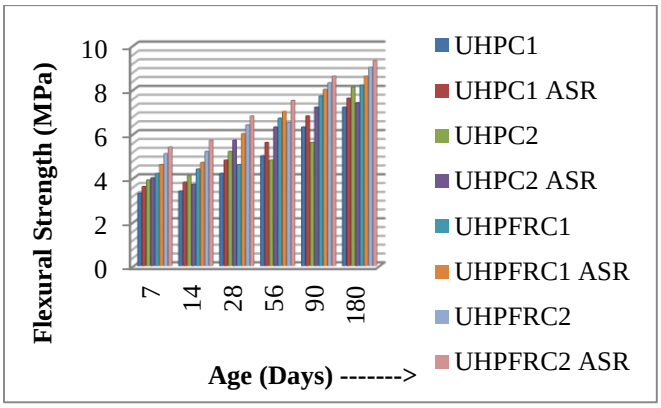

Figure 12: Split Tensile Strength

5.5 Comparison of UHPC with Normal Strength Concrete

Table 6 compares the Mechanical Strength (MS) of UHPFRC and NSC over curing periods of 28, 56, and 90 days, focusing on the effects of ASR and water curing. For CS, UHPFRC exhibits significantly higher values under both ASR and water curing, reaching up to 161MPa at 90 days compared to a maximum of 37.8MPa for NSC. This highlights UHPFRC's superior load-bearing capacity. FS, indicative of bending resistance, also favors UHPFRC, with values reaching 28.7MPa under water curing at 90 days, compared to NSC's 11.8MPa. Similarly, STS for UHPFRC remains higher across all conditions, with a peak of 10MPa at 28 days under ASR curing. NSC, by contrast, shows lower STS capacities, peaking at 5.5MPa at 28 days. The results demonstrate that ASR curing marginally enhances CS and FS for UHPFRC while showing mixed effects on tensile strength. NSC performance remains comparatively lower under all conditions, affirming UHPFRC's advanced performance due to its dense matrix and resistance to microstructural degradation. The findings underline the critical role of quality control in optimizing UHPFRC's durability and strength. Figure 13 show the comparison graph of MS outcomes for UHPC and NSC.

Table 6: Evaluation of MS outcomes for UHPC and NSC

Properties	Exposure	UHPFRC			NSC		
		28	56	90	28	56	90
Compressive Strength (MPa)	ASR	112	142	151	27.5	30.1	37.8
	Water	122	151	161	25.2	27.3	33.6
Flexural Strength (MPa)	ASR	21	25	28	8.8	10.6	11.8
	Water	22.3	25.8	28.7	8.6	9.8	10.6
Split Tensile	ASR	10	8.3	9.1	5.5	4.7	5.1

Strength (MPa)	**Water**	9.6	8.4	9.5	4.6	4.5	4.7

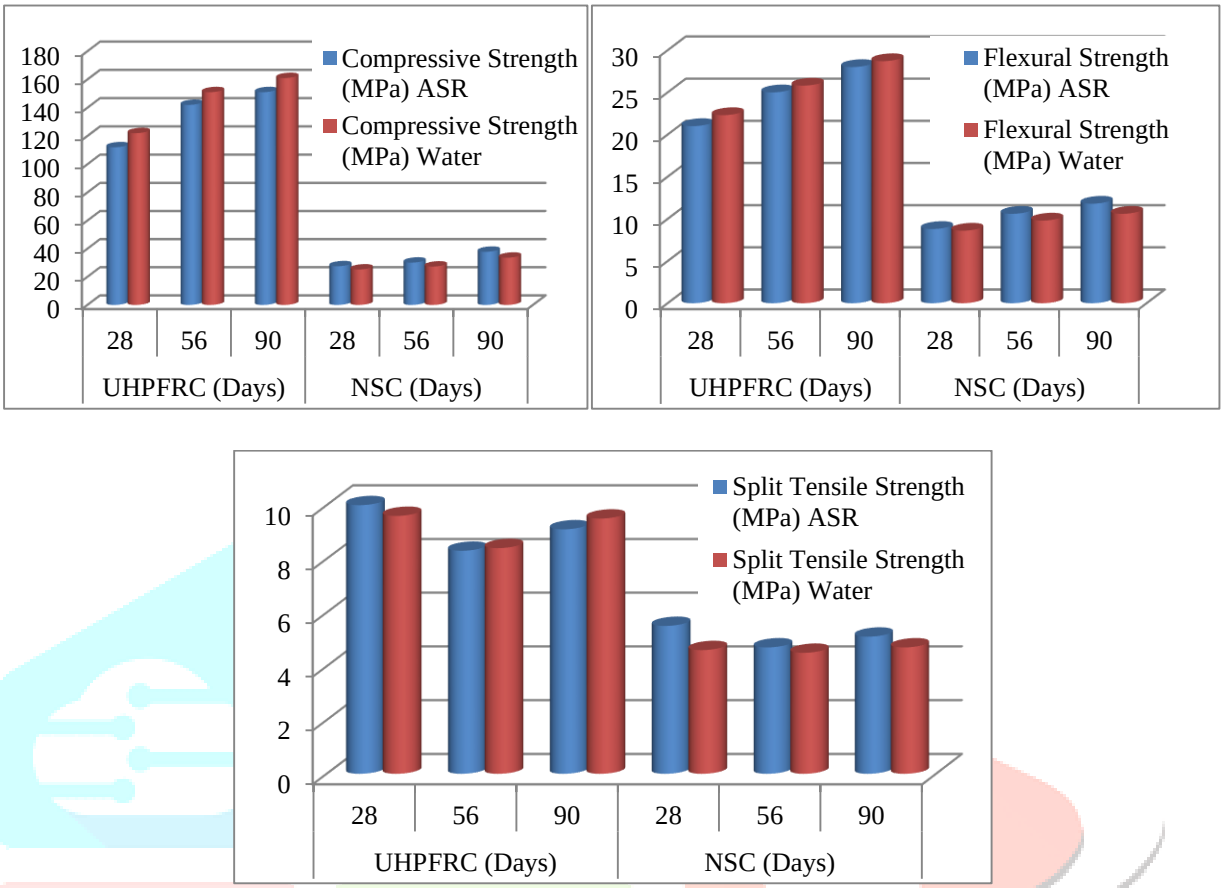

Figure 13: Comparison of MS results for UHPC and NSC

In addition, the evaluated NSC specimens showed visible surface map fractures (Figure 14 (a)), which proved the presence of expanding ASR products. The localized swelling caused by the ASR gel that forms when alkalis and reactive silica react lowers the strength characteristics of concrete and causes internal micro-cracking [42]. Conversely, it is worth noting that UHPFRC specimens subjected to ASR circumstances showed an intriguing rise in CS, indicating that the accelerated ASR exposure conditions had no major impact. Figure 14 (b) shows that none of the established UHPC specimens subjected to the accelerated ASR condition developed surface fractures.

(a) (b)

Figure 14: Surface cracks in a) NSC and b) UHPC

After28,56, and 90 days of exposure to accelerated ASR conditions, the FS of the NSC samples dropped from 8.8, 10.1, and 11.8MPa to 8.6, 9.8, and 10.6MPa, respectively. The primary reason of the reduction in FS that happened after being exposed to ASR was the increased tensile strains caused by the ASR gel expanding [43]. However, in accelerated ASR circumstances, UHPC specimens showed a rise in FS, which is comparable to compressive strength. Because more CSH products are formed at higher temperatures, the microstructure of UHPC exposed to accelerated ASR conditions becomes denser, which in turn increases the mechanical strength qualities [44].

6. Conclusion

The study on ASR in UHPC highlights the critical need for effective performance evaluation and quality control measures to ensure durability and long-term structural reliability. UHPC and its UHPFRC demonstrate exceptional mechanical properties, including high CS, FS, and STS. However, the dense matrix and high cement content in UHPC increase its susceptibility to ASR, which can compromise durability through cracking and expansion. The current research investigated the mechanical and durability properties of environmentally friendly UHPC blends using CA and RS, as well as locally recycled steel fibers, in water and under accelerated ASR conditions. In addition, they compared the UHPC mixes' performance to that of NSC. A few conclusions can be taken from the experimental data:

- Fiber-reinforced mixtures, especially UHPFRC2, exhibited superior performance across all strength categories, with CS reaching up to 164MPa at 108 days and FS up to 29MPa, showing an impressive improvement over the non-fiber reinforced variants. This highlights the synergistic effect of fiber reinforcement and optimized mix design in achieving exceptional strength, especially at later curing ages.

- UHPFRC2 exhibited the lowest ASR expansion, maintaining an expansion of just 0.013% at 108 days, contrasting with the higher expansions observed in the non-fiber mixes, which were 0.13% for UHPC1 and 0.126% for UHPC2.
- The comparison with NSC further underscored the advantages of UHPC and UHPFRC, which consistently outperformed NSC across all strength categories, with CS reaching up to 161MPa at 90 days compared to the maximum 37.8MPa for NSC. This clearly demonstrates the exceptional load-bearing capacity and resistance to microstructural degradation of UHPC, making it a highly promising material for demanding structural applications.

Reference

1. Elshazli, Mohamed T., Nick Saras, and Ahmed Ibrahim. "Structural response of high strength concrete beams using fiber reinforced polymers under reversed cyclic loading." Sustain. Struct 2, no. 2 (2022): 000018.
2. Elshazli, Mohamed T., Kevin Ramirez, Ahmed Ibrahim, and Mohamed Badran. "Mechanical, durability and corrosion properties of basalt fiber concrete." Fibers 10, no. 2 (2022): 10.
3. Almakrab, Abdullah, Mohamed T. Elshazli, Ahmed Ibrahim, and Yasser A. Khalifa. "Assessment of Various Mitigation Strategies of Alkali-Silica Reactions in Concrete Using Accelerated Mortar Test." Materials 17, no. 20 (2024): 5124.
4. Rajabipour, Farshad, Eric Giannini, Cyrille Dunant, Jason H. Ideker, and Michael DA Thomas. "Alkali–silica reaction: Current understanding of the reaction mechanisms and the knowledge gaps." Cement and Concrete Research 76 (2015): 130-146.
5. Aquino, W., D. A. Lange, and J. Olek. "The influence of metakaolin and silica fume on the chemistry of alkali–silica reaction products." Cement and Concrete Composites 23, no. 6 (2001): 485-493.
6. Zapała-Sławeta, Justyna. "Alkali silica reaction in the presence of metakaolin-the significant role of calcium hydroxide." In IOP Conference Series: Materials Science and Engineering, vol. 245, no. 2, p. 022020. IOP Publishing, 2017.
7. Elshazli, Mohamed T., Ahmed Ibrahim, Elmar Eidelpes, and Gabriel O. Ilevbare. "Degradation mechanisms in overpack concrete of spent nuclear fuel dry storage systems: A review." Nuclear Engineering and Design 414 (2023): 112632.
8. Olajide, Olusola D., Michelle R. Nokken, and Leandro FM Sanchez. "Alkali–Silica Reactions: Literature Review on the Influence of Moisture and Temperature and the Knowledge Gap." Materials 17, no. 1 (2023): 10.
9. Ichikawa, Tsuneki, and Masazumi Miura. "Modified model of alkali-silica reaction." Cement and Concrete research 37, no. 9 (2007): 1291-1297.

10. Thomas, M. D. A., Benoît Fournier, and Kevin J. Folliard. Selecting measures to prevent deleterious alkali-silica reaction in concrete: rationale for the AASHTO PP65 prescriptive approach. No. FHWA-HIF-13-002. United States. Federal Highway Administration, 2012.

11. Godart, Bruno, Mario Robert de Rooij, and Jonathan GM Wood. Guide to diagnosis and appraisal of AAR damage to concrete in structures. Berlin: Springer, 2013.

12. Fanijo, Ebenezer O., John Temitope Kolawole, and Abdullah Almakrab. "Alkali-silica reaction (ASR) in concrete structures: Mechanisms, effects and evaluation test methods adopted in the United States." Case Studies in Construction Materials 15 (2021): e00563.

13. Thomas, Michael DA, Benoit Fournier, Kevin J. Folliard, and Yadhira Resendez. Alkali-silica reactivity field identification handbook. No. FHWA-HIF-12-022. United States. Federal Highway Administration. Office of Pavement Technology, 2011.

14. Saha, Ashish Kumer, Md Nabi Newaz Khan, Prabir Kumar Sarker, Faiz Ahmed Shaikh, and Alokesh Pramanik. "The ASR mechanism of reactive aggregates in concrete and its mitigation by fly ash: A critical review." Construction and Building Materials 171 (2018): 743-758.

15. Lima, Mehdi, R. Salamy, and D. Miller. "CFRP strengthening of ASR affected concrete piers of railway bridges." In Maintenance, Safety, Risk, Management and Life-Cycle Performance of Bridges, pp. 346-353. CRC Press, 2018.

16. Salamy, R., M. Lima, and D. Miller. "Rehabilitation and CFRP strengthening of ASR affected concrete bridge piers." In 5th fib Congress, FIB 2018, pp. 3896-3903. 2019.

17. Demir Şahin, Demet. "Evaluation of Cherts in Gumushane Province in Terms of Alkali Silica Reaction." Buildings 14, no. 4 (2024): 873.

18. Snyder, Kenneth A., and Hai S. Lew. "Alkali-silica reaction degradation of nuclear power plant concrete structures: A scoping study." National Institute of Standards and Technology (NIST), US Department of Commerce, Document ID-NISTIR 7937 (2013).

19. Azmee, Norzaireen Mohd, and Nasir Shafiq. "Ultra-high performance concrete: From fundamental to applications." Case Studies in Construction Materials 9 (2018): e00197.

20. Camacho Torregrosa, Esteban Efraím. "Dosage optimization and bolted connections for UHPFRC ties." PhD diss., Universitat Politècnica de València, 2014.

21. Amran, Mugahed, Shan-Shan Huang, Ali M. Onaizi, Natt Makul, Hakim S. Abdelgader, and Togay Ozbakkaloglu. "Recent trends in ultra-high performance concrete (UHPC): Current status, challenges, and future prospects." Construction and Building Materials 352 (2022): 129029.

22. Zheng, Dong, Ali H. AlAteah, Ali Alsubeai, and Sahar A. Mostafa. "Integrating micro-and nanowaste glass with waste foundry sand in ultra-high-performance concrete to enhance material performance and sustainability." Reviews on Advanced Materials Science 63, no. 1 (2024): 20240012.

23. Qin, Jihui, Zhichao Zhang, Hongyan Ma, Xiaobing Dai, Xing Cheng, Xingwen Jia, and Jueshi Qian. "Improving mechanical properties of magnesium phosphate cement-based ultra-high performance concrete by ultrafine fly ash incorporation." Construction and Building Materials 448 (2024): 138198.

24. Mousavinezhad, Seyedsaleh, Gregory J. Gonzales, William K. Toledo, Judit M. Garcia, Craig M. Newtson, and Srinivas Allena. "A Comprehensive Study on Non-Proprietary Ultra-High-Performance Concrete Containing Supplementary Cementitious Materials." Materials 16, no. 7 (2023): 2622.

25. Abdellatief, Mohamed, Saeeb M. Al-Tam, Walid E. Elemam, Hani Alanazi, Gamal M. Elgendy, and Ahmed M. Tahwia. "Development of ultra-high-performance concrete with low environmental impact integrated with metakaolin and industrial wastes." Case Studies in Construction Materials 18 (2023): e01724.

26. Glanz, Dilan, Husam Sameer, Daniela Göbel, Alexander Wetzel, Bernhard Middendorf, Clemens Mostert, and Stefan Bringezu. "Comparative environmental footprint analysis of ultra-high-performance concrete using Portland cement and alkali-activated materials." Frontiers in Built Environment 9 (2023): 1196246.

27. Amin, Mohamed, Ibrahim Y. Hakeem, Abdullah M. Zeyad, Bassam A. Tayeh, Ahmed M. Maglad, and Ibrahim Saad Agwa. "Influence of recycled aggregates and carbon nanofibres on properties of ultra-high-performance concrete under elevated temperatures." Case Studies in Construction Materials 16 (2022): e01063.

28. Aisheh, Yazan Issa Abu, Dawood Sulaiman Atrushi, Mahmoud H. Akeed, Shaker Qaidi, and Bassam A. Tayeh. "Influence of steel fibers and microsilica on the mechanical properties of ultra-high-performance geopolymer concrete (UHP-GPC)." Case Studies in Construction Materials 17 (2022): e01245.

29. ASTM C1260. Standard Test Method for Potential Alkali Reactivity of Aggregates (Mortar-Bar Method); American Society for Testing Materials: West Conshohocken, PA, USA, 2014; p. 5.

30. Babalu, Rajput, Agarwal Anil, Kore Sudarshan, and Pawar Amol. "Compressive strength, flexural strength, and durability of high-volume fly ash concrete." Innovative Infrastructure Solutions 8, no. 5 (2023): 154.

31. Mydin, M. A. O., N. Md Sani, MA Mohd Yusoff, and S. Ganesan. "Determining the compressive, flexural and splitting tensile strength of silica fume reinforced lightweight foamed concrete." In MATEC Web of Conferences, vol. 17, p. 01008. EDP Sciences, 2014.

32. Harish, B. A., B. M. Hanumesh, T. M. Siddesh, and B. Siddhalingesh. "An experimental investigation on partial replacement of cement by glass powder in concrete." Int. Res. J. Eng. Technol 3, no. 10 (2016).

33. Jadhav, Sandesh, and Rahul S. Patil. "Comparison of flexural, split tensile & compressive strength of HP-SCC using magnetized water." International Journal of Emerging Trends in Engineering Research 4 (2016): 130-135.

34. https://testbook.com/civil-engineering/splitting-tensile-test-of-concrete

35. ASTM C230. Standard Specification for Flow Table for Use in Tests of Hydraulic Cement; American Society for Testing Materials: West Conshohocken, PA, USA, 2021; p. 7.

36. ASTM C109. Standard Test Method for Compressive Strength of Hydraulic Cement Mortars (Using 2-in. or [50 mm] Cube Specimens); American Society for Testing Materials: West Conshohocken, PA, USA, 2020; p. 12.

37. ASTM C348. Standard Test Method for Flexural Strength of Hydraulic-Cement Mortars; American Society for Testing Materials: West Conshohocken, PA, USA, 2020; p. 6.

38. ASTM C490 Standard Practice for Use of Apparatus for the Determination of Length Change of Hardened Cement Paste, Mortar, and Concrete; American Society for Testing Materials: West Conshohocken, PA, USA, 2017; p. 5.

39. Abbas, Safeer, Uzair Arshad, Wasim Abbass, Moncef L. Nehdi, and Ali Ahmed. "Recycling untreated coal bottom ash with added value for mitigating alkali–silica reaction in concrete: A sustainable approach." Sustainability 12, no. 24 (2020): 10631.

40. Grunewald, S. "Performance based design of self compacting steel fiber reinforced concrete." Delft University of Technology (2004).

41. Boulekbache, Bensaid, Mostefa Hamrat, Mohamed Chemrouk, and Sofiane Amziane. "Flowability of fibre-reinforced concrete and its effect on the mechanical properties of the material." Construction and Building Materials 24, no. 9 (2010): 1664-1671.

42. Abbas, Safeer, Syed MS Kazmi, and Muhammad J. Munir. "Potential of rice husk ash for mitigating the alkali-silica reaction in mortar bars incorporating reactive aggregates." Construction and Building Materials 132 (2017): 61-70.

43. Abbas, Safeer, Ali Ahmed, Moncef L. Nehdi, Danish Saeed, Wasim Abbass, and Faisal Amin. "Eco-friendly mitigation of alkali-silica reaction in concrete using waste-marble powder." Journal of Materials in Civil Engineering 32, no. 9 (2020): 04020270.

44. Hassan, A. M. T., G. H. Mahmud, A. S. Mohammed, and S. W. Jones. "The influence of normal curing temperature on the compressive strength development and flexural tensile behaviour of UHPFRC with vipulanandan model quantification." In Structures, vol. 30, pp. 949-959. Elsevier, 2021.